Received 13 December 2021; revised 1 February 2022; accepted 6 February 2022. Date of publication 11 February 2022; date of current version 1 March 2022.
The review of this article was arranged by Editor C. Bulucea

Digital Object Identifier 10.1109/JEDS.2022.3150915

High-Temperature Piezoresistance of Silicon Carbide and Gallium Nitride Materials

TAKAYA SUGIURA [1] (Member, IEEE), NAOKI TAKAHASHI [1], RYOHEI SAKOTA [1], KAZUNORI MATSUDA [2], AND NOBUHIKO NAKANO [1] (Member, IEEE)

1 Department of Electronics and Electrical Engineerings, Keio University, Yokohama 223-8522, Japan
2 Department of Nano Material and Bio Engineering, Tokushima Bunri University, Sanuki 769-2193, Japan

CORRESPONDING AUTHOR: T. SUGIURA (e-mail: takaya_sugiura@nak.elec.keio.ac.jp)

ABSTRACT We examine the temperature dependence of the piezoresistive coefficients of silicon carbide (SiC) and gallium nitride (GaN) crystals, which are prospective materials for high-temperature applications owing to their wide-bandgap properties. The temperature-dependent piezoresistive coefficients of these materials were obtained by modeling experimental resistance changes using thermomechanical numerical simulations. This work reports the piezoresistive coefficients of 4H-SiC and GaN at the high-temperature environments, which are still not well researched. The results revealed that the temperature dependences of piezoresistive coefficients were strongly related to the ionization energy, and a high ionization energy stabilized the values of the piezoresistive coefficients at high temperatures. Our proposed temperature modeling method helps in predicting the temperature dependence of the piezoresistive coefficient using the value at the room temperature and the ionization energy of the material, which is useful for evaluating the piezoresistive effect at different temperatures during device simulations.

INDEX TERMS Device simulation, ionization energy, piezoresistive effect, temperature dependence, wide band-gap semiconductors.

I. INTRODUCTION

The piezoresistive effect of certain materials is observed as a change in their relative resistivity under the application of stress. This piezoresistive property is exploited in stress/strain sensor applications because it affords high sensitivity and varies suitably linearly against the applied stress. In particular, semiconductor materials show significantly larger piezoresistivity changes than those exhibited by metals; for semiconductors, the gauge factor (GF), defined as the ratio of the relative resistivity change to the applied strain, is several tens of times larger than those of metals, reaching ∼100 for Si (silicon) material. Furthermore, we remark that the piezoresistive coefficient, which is a unique physical constant of a material that expresses the magnitude and sign of the piezoresistive effect, has been found to decrease with an increase in temperature [1].

Conventional Si materials are widely used in piezoresistive applications; however, their applicability is limited under extreme conditions such as high temperatures or chemically corrosive environments. At the basic piezoresistor structure that forms over the doped-substrate, the temperature robustness until 150 °C is ensured; means that the silicon-only has the low temperature robustness and enhancing it needs the combination of dielectric passivation such as oxide [2]. Meanwhile, wide-bandgap materials such as silicon carbide (SiC) and gallium nitride (GaN) are being considered as candidate materials for piezoresistive applications [3]. In particular, SiC materials exhibit a significant high-temperature robustness, withstanding temperatures of over 600 °C. With regard to the application perspective, it is particularly important to understand the physics of the material under high temperatures; in this regard, some studies have focused on the temperature dependences of the piezoresistive coefficients of SiC and GaN, with experiments estimating the GF values in lieu of the piezoresistivity performance [4], [5]. Meanwhile, with regard to numerical simulations, the piezoresistive coefficient plays an important role in the evaluation of the piezoresistive effect, and in a

previous work, we proposed piezoresistive mobility modeling using the longitudinal- and transverse-direction piezoresistive coefficients [6]. Based on the above study, we note that to evaluate the piezoresistive effect at high temperatures, the input piezoresistive coefficients should be modified; thus, the temperature dependence of these coefficients plays a significant part in the evaluation.

Against this backdrop, in this study, we report on the temperature dependences of the piezoresistive coefficients of SiC and GaN crystals. The temperature dependences of the piezoresistive coefficients were derived from the numerical simulation that reproduced the experimental results reported for SiC and GaN. Our piezoresistive coefficient modeling includes the temperature term, which is determined based on the GF values reported using our original device simulator that evaluates the piezoresistive effect using the longitudinal and transverse piezoresistive coefficients. In the study, we applied a linear approximation of the piezoresistive coefficient as a function of the temperature to evaluate the temperature dependence of the piezoresistive coefficients of SiC and GaN.

II. UNDERLYING PHYSICS

A. PIEZORESISTIVE MOBILITY MODELING

In our previous work, we modeled the piezoresistive effect as the mobility change in our device simulations [6]. The conventional piezoresistive model, which is mainly applicable to cubic crystal materials, is based on the piezoresistive coefficient tensor components π_{11}, π_{12}, and π_{44}, which reflect the mobility enhancement [7]. To evaluate the piezoresistive effect, we determine the stressed mobility $\mu_{Piezo_{l,t}}$ using the non-stressed mobility μ_0, the longitudinal and transverse piezoresistive coefficients, and stresses. To increase the accuracy of estimation, we consider the unique modification factor of the material, which exhibits a piezoresistive-coefficient dependency [6]. Thus, we have

$$\mu_{Piezo_{l,t}} = \frac{a_{l,t}\pi_{l,t} + b_{l,t}}{1 + \pi_{l,t}\sigma_{l,t}}\mu_0. \tag{1}$$

Here, $\pi_{l,t}$, $\sigma_{l,t}$, and $a_{l,t}$ and $b_{l,t}$ denote the piezoresistive coefficient, stress, and modification factors, respectively. This model reduces the GF errors from the GF values of the experimental results by employing the unique coefficients of the materials through empirical fitting of the experimental results. The model is proposed for general application to device simulations to evaluate the semiconductor device performance under stressed conditions.

B. PIEZORESISTIVE EFFECT OF WIDE-BANDGAP SEMICONDUCTORS

Wide-bandgap materials are considered promising candidates to replace conventional Si materials because of their prospective material properties, which afford the desirable traits of a high breakdown voltage, high operating temperature, and high Baliga's figure-of-merit [8]–[11]. In this regard, several studies have been conducted on the piezoresistivity applications of wide-bandgap materials in general. The most well-researched material is SiC, which shows a particularly large high-temperature robustness, withstanding temperatures of over 600 °C, and excellent material properties such as high chemical stability and a large Young's modulus [3]. Meanwhile, GaN is considered as another promising wide-bandgap material. Although GaN exhibits a smaller Young's modulus and a lower application-temperature range relative to the counterpart SiC values, its larger electron affinity of N atoms induces polarization, which plays a significant role in the piezoelectric effect [12]. Furthermore, it has been reported that GaN materials can potentially exhibit GF values as large as ∼130 as a transient characteristic due to the piezoelectric polarization effect [13]

TABLE 1. Physical phenomena considered in the simulation.

Simulation type	Physics
Electrical [6]	Piezoresistive effect
	Incomplete ionization [17]
Mechanical [18]	Solid dynamics
	Heat transfer
	Thermal expansion (Multiphysics)

C. PIEZORESISTIVE COEFFICIENT VARIATIONS DUE TO EXTERNAL EFFECTS

The piezoresistive coefficient decreases as the temperature increases, as reported by Richter *et al.* [14]. It has been reported that a higher temperature and higher dopant concentration reduce the piezoresistive coefficient [15]. The piezoresistance phenomenon is based on the band theory, and the band-gap energy is affected by the temperature; the increased temperature decreases the band-gap energy [16]. Moreover, crystallographic misalignment is known to influence the effective piezoresistive coefficient, and for Si materials, the dopant type affects the misalignment. Parameters such as π_{11} and π_{12} are sensitive to the degree of misalignment for p-doped Si, whereas π_{44} is sensitive to misalignment in the case of n-doped Si. A higher piezoresistive coefficient is required for high-sensitivity sensor applications. Furthermore, it must be noted that the material robustness to the temperature differs among materials. For example, SiC materials maintain high GF values even at extremely high temperatures of approximately 600 °C [4], [19]. In contrast, GaN exhibits a GF drop of nearly 50% at approximately 100 °C [5]; this makes SiC materials sui candidates for high-temperature mechanical-sensing applications.

III. SIMULATION MODEL

Our simulations were modeled with 2D components, which were composed of mechanical stress and electrical simulations. Figure 1 shows the schematic of the numerical simulation modeling adopted in this study for SiC and GaN materials. Table 1 lists the relevant physical phenomena for the mechanical and electrical simulations considered in this study. For temperature modeling, the band-gap temperature

TABLE 2. Simulation modeling of 4H-SiC.

Physics	Value
Crystal plane [20]	(0001)
Young's modulus E **[GPa]** [21]	503.7
Poisson's ratio γ [22]	0.16
Thermal expansion coefficient α_T **[1/°C]** [23]	$\alpha_{11} = 3.21 \times 10^{-6} + 3.56 \times 10^{-9}T - 1.62 \times 10^{-12}T^2$, $\alpha_{33} = 3.09 \times 10^{-6} + 2.63 \times 10^{-9}T - 1.08 \times 10^{-12}T^2$
Bandgap energy E_{g0} **[eV]** [24]	3.29
Bandgap energy parameter α **[eV/K]** [24]	3.30×10^{-2}
Bandgap energy parameter β **[K]** [24]	1×10^{5}
Doping concentration N_a **[cm^{-3}]** [20]	1×10^{18} (p-type)
Ionization energy [meV] [25]	200
Temperature dependence of mobility [26]	$(T/300)^{-2.4}$

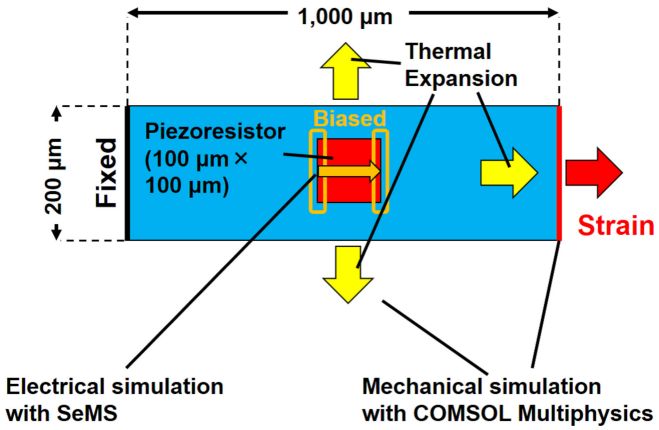

FIGURE 1. Schematic of mechanical and electrical simulation modeling considered in this study.

model [16] is used that expressed as

$$E_g(T) = E_{g0} - \alpha \frac{T^2}{\beta + T}. \tag{2}$$

Here, E_{g0} is the band-gap energy at the low-temperature, α and β are the band-gap temperature parameters with the units of eV, eV/K and K, respectively. For temperature modeling of the fundamental semiconductor properties, we introduced the temperature dependencies of density-of-state (DOS) $N_{C,V}$ as

$$N_{C,V} = 2\left(\frac{2\pi m_{e,h} kT}{h^2}\right)^{1.5}. \tag{3}$$

Then, the intrinsic carrier concentration as the temperature function is expressed as

$$n_i = n_{i,300K} \frac{\exp\left(-\frac{qE_g(T)}{2kT}\right)}{\exp\left(-\frac{qE_g(T_0)}{2kT_0}\right)} \left(\frac{T}{T_0}\right)^{1.5}. \tag{4}$$

Here, the T_0 corresponds to 300 K. The temperature dependencies are concentrated on $N_{C,V}$ and n_i. For wide-bandgap semiconductors, incomplete ionization is important, especially for SiC materials [17]. Meanwhile, the mechanical stress simulation considers the associated thermal expansion and stress. The strain by an external force was applied to the cantilever region, where a piezoresistor with dimensions of 100 μm × 100 μm was positioned at the center. The width was 1 μm along the z-direction under all conditions.

In our study, the stress simulation was performed with COMSOL Multiphysics Ver. 5.5 [18], using the solid dynamics and heat transfer modules with multiphysics analysis. In the simulation, thermal expansion was considered, and a mechanical strain was applied to the edge of the cantilever region. The temperature was varied according to previously reported piezoresistive experiments. The strain of the piezoresistor was calculated as the difference between the final strain and the thermal expansion strain (no external force). In addition, the resistance change of the piezoresistor was calculated as the difference between the resistance under the final strain condition and that under the thermal expansion strain condition (no external force). In our study, the electrical simulation was performed with the use of our original device simulator, called SeMS [6], and was customized for evaluating piezoresistor performance. Subsequently, in the simulation, a voltage bias of 1 V $\rightarrow$ -1 V was applied to obtain the I–V characteristics. The input piezoresistive coefficient and the temperature were varied to obtain the matching GF values reported in the experiments.

IV. SIMULATION RESULTS

A. MODELING OF MATERIALS

A.1. 4H-SIC (P-TYPE)

We examined the characteristics of p-type 4H-SiC with a dopant concentration of 1×10^{18} cm^{-3} along the longitudinal direction for temperatures up to 600 °C. Table 2 lists the relevant modeling parameters used for 4H-SiC. The mechanical parameters listed in Table 2 are those observed in the (0001) plane.

First, we evaluated the accuracy of the simulation modeling by comparing to the experimental result of p-type 4H-SiC at the room temperature (23 °C). Figure 2 shows the strain–resistance change characteristic at 23 °C with the input piezoresistive coefficient of 6.43×10^{-11} Pa^{-1} and -5.12×10^{-11} Pa^{-1}, which were reported as the longitudinal and the transverse piezoresistive coefficient (π_{11} and π_{12}) at the room temperature for p-type 4H-SiC [20]. The GF value obtained from the simulation output was 33.23 and -26.46, which matched well with the experimental result [4], [21].

A.2. 6H-SIC (N-TYPE)

The relevant modeling parameters of n-type 6H-SiC are listed in Table 3. The n-type 6H-SiC in (0001) plane with both the

TABLE 3. Simulation modeling of 6H-SiC.

Physics	Value
Crystal plane [27]	(0001)
Young's modulus E **[GPa]** [28]	488
Poisson's ratio γ [18]	0.45
Thermal expansion coefficient α_T **[1/°C]** [29]	$\alpha_{11} = 3.27 \times 10^{-6} + 3.25 \times 10^{-9}T - 1.36 \times 10^{-12}T^2$, $\alpha_{33} = 3.18 \times 10^{-6} + 2.48 \times 10^{-9}T - 8.51 \times 10^{-13}T^2$
Bandgap energy E_{g0} **[eV]** [16]	3.024
Bandgap energy parameter α **[eV/K]** [16]	-3.06×10^{-5}
Bandgap energy parameter β **[K]** [16]	-311
Doping concentration N_d **[cm^{-3}]** [27]	3×10^{19} (n-type)
Ionization energy [meV] [30], [31]	45
Temperature dependence of mobility [26]	$(T/300)^{-2.5}$

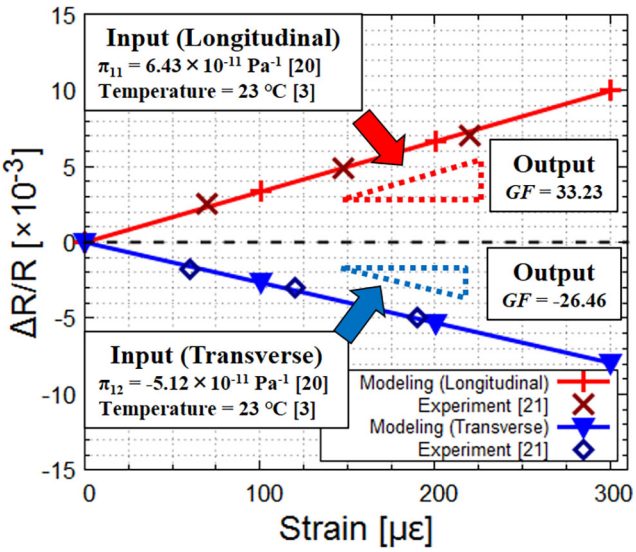

FIGURE 2. Δ/R/R versus strain of p-type 4H-SiC with the input piezoresistive coefficient of 6.43 × 10^{-11} Pa^{-1} at 23 °C and comparison to the experimental results [20].

TABLE 4. Simulation modeling of 3C-SiC.

Physics	Value
Crystal direction [32]	<100>
Young's modulus E **[GPa]** [33]	330
Poisson's ratio γ [34]	0.267
Thermal expansion coefficient α_T **[1/K]** [35]	$5 \times 10^{-9}T + 2 \times 10^{-6}$
Bandgap energy E_{g0} **[eV]** [24]	2.39
Bandgap energy parameter α **[eV/K]** [24]	6.00×10^{-3}
Bandgap energy parameter β **[K]** [24]	1,200
Doping concentration N_d **[cm^{-3}]** [32]	1×10^{18}, 1×10^{20} (n-type)
Ionization energy [meV] [36]	54.2
Temperature dependence of mobility [26]	$(T/300)^{-2.5}$

TABLE 5. Simulation modeling of GaN.

Physics	Value
Crystal plane [5]	(0001)
Young's modulus E **[GPa]** [37]	295
Poisson's ratio γ [38]	0.183
Thermal expansion coefficient α_T **[1/K]** [39]	$\alpha = 3.7 \times 10^{-6}$
Bandgap energy E_{g0} **[eV]** [40]	3.51
Bandgap energy parameter α **[eV/K]** [40]	9.09×10^{-4}
Bandgap energy parameter β **[K]** [40]	830
Doping concentration N_d **[cm^{-3}]** [5]	1×10^{18} (n-type)
Ionization energy [meV] [41], [42]	17
Temperature dependence of mobility [43]	$(T/300)^{-1.5}$

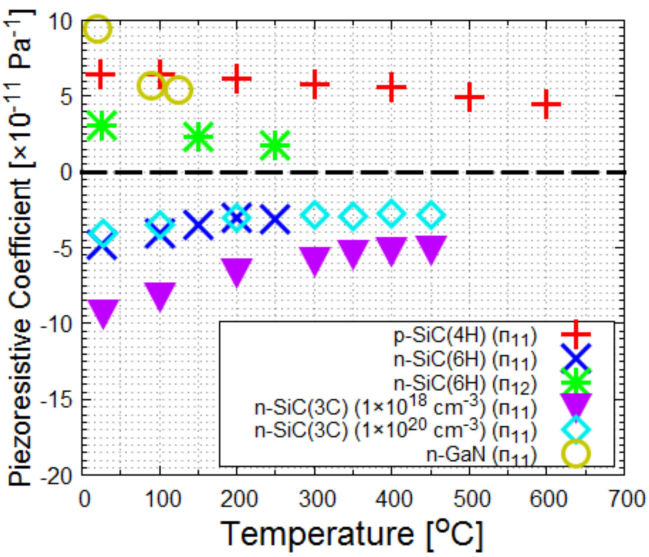

FIGURE 3. Piezoresistive coefficient value of materials as a function of temperature.

longitudinal and the transverse direction of 3×10^{19} cm^{-3} are evaluated up to 250 °C [27].

A.3. 3C-SIC (N-TYPE)

The relevant modeling parameters of n-type 3C-SiC are listed in Table 4. The n-type 3C-SiC in<100> direction with two doping concentrations of 1×10^{18} and 1×10^{20} cm^{-3} were evaluated up to 450 °C [32].

A.4. GAN (N-TYPE)

The relevant modeling parameters of n-type GaN are listed in Table 5. In this study, an epitaxial GaN layer was used as the piezoresistor considering a previous study [5], and the (0001) plane was considered. The mechanical parameters corresponded to those in the (0001) plane. We evaluated the piezoresistive characteristics of n-type GaN with a dopant concentration of 1×10^{18} cm^{-3} along the longitudinal direction up to a temperature of 125 °C.

B. PIEZORESISTIVE COEFFICIENT VERSUS TEMPERATURE

Figure 3 shows the piezoresistive coefficients as functions of the temperature of materials. For all materials, the high temperature decreased the coefficient; however, the response to temperature differed. A major difference was observed

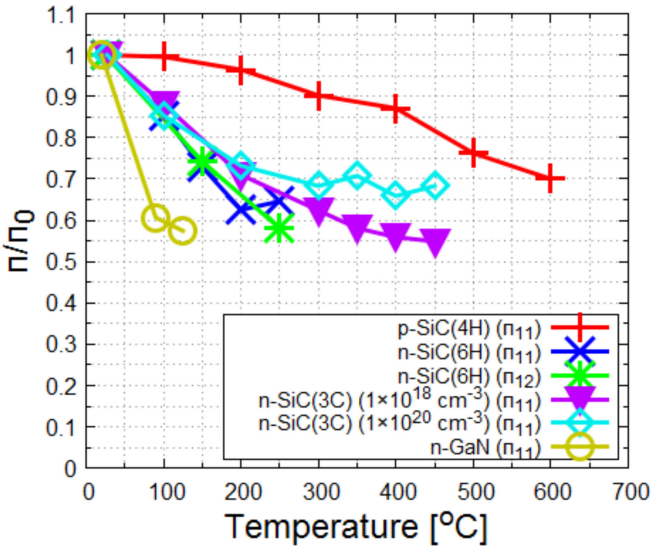

FIGURE 4. Piezoresistive coefficient ratio of materials as a function of temperature.

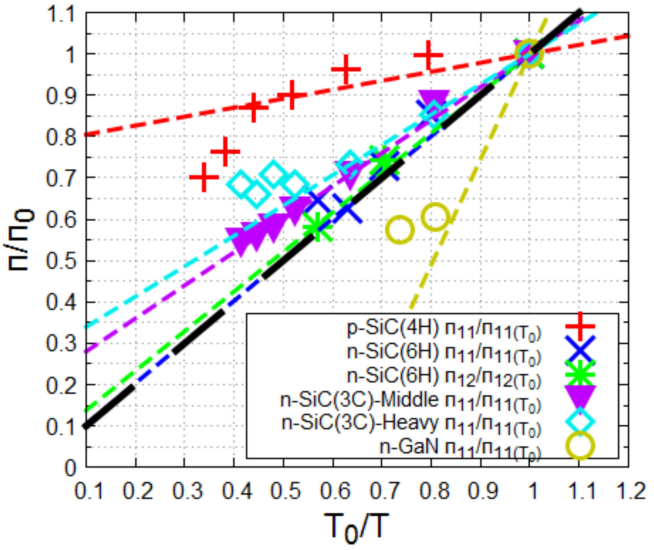

FIGURE 5. Proposed piezoresistive temperature modeling with the comparison to the fittings of the piezoresistive temperature dependencies.

between the p-type and the n-type materials. In p-type 4H-SiC, a relatively stabilized value was obtained until 400 °C and the value decreased thereafter. On the contrary, the n-type materials provided larger drops at the when the temperature increased from the room temperature, and it then stabilized at the higher temperature region. Figure 4 shows the ratio of the piezoresistive coefficient for each temperature to the value at the room temperature to clarify the trends. In n-type 6H-SiC, only the π_{12} was difficult to observe the inflection; however, the slight inflection seems to occur between the temperature of 150 °C to 250 °C considering the result of Toriyama's calculation [27].

V. DISCUSSION

Upon comparing the piezoresistive temperature models of SiC and GaN, we note that SiC exhibits a smaller sensitivity to temperature. In contrast, GaN exhibits a rapid change in the GF against the temperature; an approximate increase of 100 K corresponds to a decrease of >10 in terms of the absolute GF value. However, for SiC, a GF decrease by 10 corresponds to a temperature increase of approximately 600 K. This result indicates that SiC materials afford high-temperature robustness and high sensitivity at high temperatures, which makes them suitable for piezoresistive sensing applications.

Richter *et al.* have reported that the piezoresistive coefficient varies linearly with a temperature ratio of 'T_0/T' [14]. Richter *et al.* reported that the ratio of the piezoresistive coefficient $\pi_{44}/\pi_{44(300K)} = 300/T$ at the region of $0.8 < 300/T < 1$ [14]; we apply this linear approximation to the results of materials. The linear approximation is taken as

$$\frac{\pi}{\pi_0} = a_{mat}\left(\frac{T_0}{T}\right) + 1 - a_{mat}. \tag{5}$$

TABLE 6. Linear approximation expressions of the temperature dependence of materials shown in Fig. 5.

Material	Expression
p-type Si [14]	$\frac{\pi}{\pi_0} = \frac{T_0}{T}$
p-type 4H-SiC	$\frac{\pi}{\pi_0} = 0.217\frac{T_0}{T} + 0.783$
n-type 6H-SiC (π_{11})	$\frac{\pi}{\pi_0} = 0.996\frac{T_0}{T} + 0.004$
n-type 6H-SiC (π_{12})	$\frac{\pi}{\pi_0} = 0.958\frac{T_0}{T} + 0.042$
n-type 3C-SiC (Middle doped)	$\frac{\pi}{\pi_0} = 0.8\frac{T_0}{T} + 0.2$
n-type 3C-SiC (Heavy doped)	$\frac{\pi}{\pi_0} = 0.734\frac{T_0}{T} + 0.266$
n-type GaN	$\frac{\pi}{\pi_0} = 2.55\frac{T_0}{T} - 1.55$

Here, for p-type Si, the a_{Si} of the a_{mat} of p-type Si is 1.

Figure 5 shows the linear approximation of the piezoresistive coefficient ratio against the temperature ratio of T_0/T for materials. As mentioned in the previous section, all the p-type 4H-SiC, n-type 6H-SiC, n-type 3C-SiCs and n-type GaN showed variation in the piezoresistive coefficient at high temperature. Therefore, the linear approximation was applicable up to the middle temperature region (before the variation) Linear approximation of each material is summarized in Table 6. The coefficient of the linear approximation a_{mat} is compared to the ionization energy of materials, as listed in Table 7. It is evident that the coefficients determined using the linear model are strongly related to the ionization energies of the materials, and the reciprocal of the ratio of the ionization energy of the material to the ionization energy of p-type Si is almost the same as that determined using the linear model. Therefore, the coefficients determined using the proposed linear model were calculated using the ionization energies of the materials as follows:

$$a_{mat} = \frac{E_{Si}}{E_{mat}} a_{Si}. \tag{6}$$

TABLE 7. Comparison of the coefficients of all materials used in the model.

Material	p-type Si	p-type 4H-SiC	n-type 6H-SiC	n-type 3C-SiC (Middle doped)	n-type 3C-SiC (Heavy doped)	n-type GaN
Piezoresistive coefficient tensor component	π_{44} [14]	π_{11} [4]	π_{11}, π_{12} [27]	π_{11} [32]	π_{11} [32]	π_{11} [5]
Ionization energy E_{mat} [meV]	43.3 [46]	200 [25]	45 [30], [31]	54.2 [36]	54.2 [36]	17 [41], [42]
Coefficient (from Fig.5) a_{mat}	1 [14]	0.217	0.996 (π_{11}) 0.958 (π_{12})	0.8	0.734	2.55
$1/(E_{mat}/E_{Si})$	1	0.217	0.962	0.799	0.799	2.55
T_0/T_{crit}	-	0.440	0.626 (π_{11}) 0.704 (π_{12})	0.634	-	0.807
Condition	Applicable	Applicable	Applicable	Applicable	Not Applicable (Degenerated [32])	Applicable

The linear model is based on a room temperature of 300 K; therefore, the linear model is finally expressed as

$$\frac{\pi}{\pi_0} = \frac{E_{Si}}{E_{mat}} a_{Si} \left(\frac{T_0}{T} \right) + 1 - \frac{E_{Si}}{E_{mat}} a_{Si}. \tag{7}$$

It is noted that the proposed temperature modeling assumes a higher temperature region than the room temperature RT, as reported by Richter for the temperature dependence of p-type Si [14]. Kanda reported the temperature dependence of the piezoresistive coefficient in silicon by using the piezoresistance factor $P(N, T)$ that includes the Fermi-integral as a function of the ionization energy [44]. This theory is strongly related with our proposing model that expresses the temperature dependence by the ionization energy. Herein, only the n-type 3C-SiC with doping concentration of 1×10^{20} cm^{-3} showed large error from the ionization energy. This was because of the degeneration by the heavy-doping as mentioned in the experiment and much more similar to metals than the semiconductors [32]. Therefore, we removed this from our discussion. The relationship between the ionized dopants and the carrier mobility has been discussed [46], and a high temperature ionizes more carriers from the impurity level; therefore, the contribution of the piezoresistive effect to the total resistance minimizes because the resistance owing to non-stressed mobility becomes small. The relationship between the ionization level and the piezoresistive effect has been suggested by Toriyama [27], [47], and our proposed model explains the relationship between them. Also, Sagar *et al.* reported the temperature dependence of the piezoresistive coefficient of n-type ZnSe at the low-temperature region that showed the relationship to the ionization energy [48]. The proposed temperature model states that the temperature dependence of the piezoresistive coefficient corresponds to the ionization energy of the material. Therefore, the temperature dependence of the piezoresistive coefficient can be estimated using the ratio of the ionization energy to the energy of p-type Si. Conversely, the ionization energy of a material can be determined by the temperature dependence of its piezoresistive coefficient.

Finally, we investigated the temperature dependence of the piezoresistive coefficient on the linearity, and the temperature

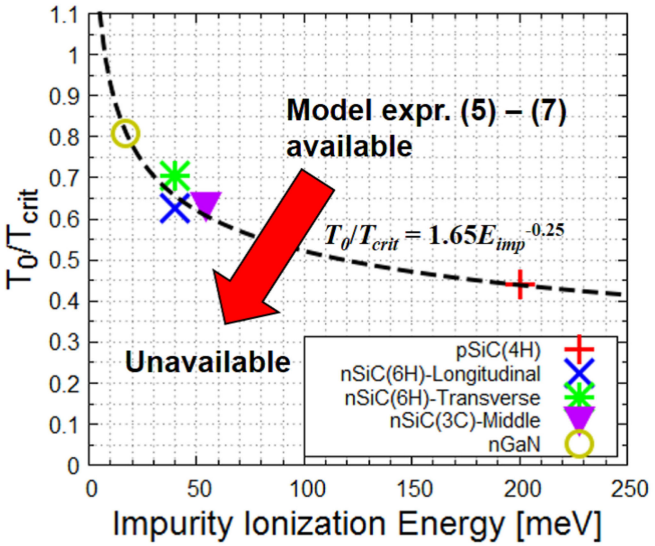

FIGURE 6. Critical temperature model against the impurity ionization energy.

was considered to be the critical temperature T_{crit}. Figure 6 shows the relationship between the impurity ionization energy and the T_0/T_{crit}. The two parameters analyzed by the model are as follows

$$\frac{T_0}{T_{crit}} = 1.65 E_{imp}^{-0.25}. \tag{8}$$

When the temperature ratio of T_0/T beyonds the interface, the temperature dependence of the piezoresistive coefficient out from the linearity, and drops for p-type or stabilizes for n-type materials, respectively. Upon combining (5) and (6), the piezoresistive coefficient can be predicted when the value at the room temperature and the ionization energy of the material are known, until the T_{crit} which follows to the linearity. The more high-temperature region can make it unavailable of the proposing models of expr. (5) and (6), however from Fig. 5 it is predicted that after the inflections the π/π_0 dependencies against T_0/T follow to the linear transitions. The extremely high-temperature region phenomena should be investigated in the future works.

The previous work suggests that the temperature dependence of the piezoresistive coefficient comes from the change

in the effective mass [49], and it is obvious that the ionization of the dopants are determined by the effective mass, as

$$E_{act} = \frac{13.6m^*}{\varepsilon_r^2 m_0}. \quad (9)$$

Here ε_r, m_0 and m^* are the dielectric constant, the electron mass and the effective mass in the semiconductor, respectively. From the temperature dependencies of the effective masses as [50]

$$\frac{m_{e,h}}{m_0} = \left(\frac{N_{C,V300K}}{2.5094 \times 10^{19}}\right)^{\frac{2}{3}} = \left(\frac{N_{C,V}\left(\frac{T}{T_0}\right)^{-\frac{3}{2}}}{2.5094 \times 10^{19}}\right)^{\frac{2}{3}}, \quad (10)$$

finally the temperature dependency of the piezoresistive coefficient can be expressed as

$$\pi = \varepsilon_r^2 \frac{43.3}{13.6}\left(\frac{N_{C,V}}{2.5094 \times 10^{19}}\right)^{-\frac{2}{3}}\left(1 - \frac{T}{T_0}\right)\pi_0. \quad (11)$$

The equation (11) expresses the piezoresistance temperature model by the fundamental band-structure parameter of the DOS. As the incomplete ionization includes the DOS (in other words the effective masses) [17], the proposing piezoresistance-temperature model connects the piezoresistance and incomplete ionization phenomenon. The proposed piezoresistive temperature model is useful to determine the ionization energy from the temperature dependence of the coefficient and vice versa. Also, for device simulation usage it is effective for inclusion of the piezoresistive effect with the temperature change.

VI. CONCLUSION

In this study, we used numerical simulations to perform temperature modeling of the piezoresistive coefficients of SiC and GaN materials. We first determined that the piezoresistive coefficients of SiC and GaN varied with temperature and higher temperatures afforded lower piezoresistive coefficients. From the response to the temperature, we found that the temperature dependence follows the ionization energy of the materials. The linear model is expressed using the ratio of the ionization energy to the ionization energy of p-type Si, which enables the estimation of the temperature dependence of the piezoresistive coefficient from the ionization energy; conversely, the ionization energy of a material can be determined from the temperature dependence of its piezoresistive coefficient. The proposed temperature dependence model can be applied to the region which it is also determined by the ionization energy. Consequently, our proposed model is useful in predicting the temperature dependence of the piezoresistive coefficient from the value obtained at the room temperature. Our model also helps in determining the ionization energy of the material. The implementation of the proposed model to device simulators will be useful for perspective materials.

ACKNOWLEDGMENT

The authors express appreciations to Assistant Prof. Hidetoshi Takahashi at Keio University, Department of Mechanical Engineering for kindly advices.

REFERENCES

[1] A. A. Barlian, W.-T. Park, J. R. Mallon, Jr., A. J. Rastegar, and B. L. Pruitt, "Review: Semiconductor piezoresistance for microsystems," *Proc. IEEE*, vol. 97, no. 3, pp. 513–552, Mar. 2009. [Online]. Available: https://doi.org/10.1109/JPROC.2009.2013612

[2] X. Li, Q. Liu, S. Pang, K. Xu, H. Tang, and C. Sun, "High-temperature piezoresistive pressure sensor based on implantation of oxygen into silicon wafer," *Sens. Actuat. A, Phys.*, vol. 179, pp. 277–282, Jun. 2012. [Online]. Available: https://doi.org/10.1016/j.sna.2012.03.027

[3] H.-P. Phan, D. V. Dao, K. Nakamura, S. Dimitrijev, and N.-T. Nguyen, "The piezoresistive effect of SiC for MEMS sensors at high temperatures: A review," *J. Microelectromech. Syst.*, vol. 24, no. 6, pp. 1663–1677, Dec. 2015. [Online]. Available: https://doi.org/10.1109/JMEMS.2015.2470132

[4] T.-K. Nguyen, H.-P. Phan, T. Dinh, A. R. M. Foisal, N.-T. Nguyen, and D. V. Dao, "High-temperature tolerance of the piezoresistive effect in p-4H-SiC for harsh environment sensing," *J. Mater. Chem. C*, vol. 6, pp. 8613–8617, Jul. 2018. [Online]. Available: https://doi.org/10.1039/C8TC03094D

[5] V. Tilak, A. Vertiatchikh, J. Jiang, N. Reeves, and S. Dasgupta, "Piezoresistive and piezoelectric effects in GaN," *Physica Stattus Solidi C*, vol. 3, no. 6, pp. 2307–2311, Jun. 2006. [Online]. Available: https://doi.org/10.1002/pssc.200565217

[6] T. Sugiura, N. Takahashi, and N. Nakano, "The piezoresistive mobility modeling for cubic and hexagonal silicon carbide crystals," *J. Appl. Phys.*, vol. 127, no. 24, Jun. 2020, Art. no. 245113. [Online]. Available: https://doi.org/10.1063/5.0006830

[7] K. Matsuda, K. Suzuki, K. Yamamura, and Y. Kanda, "Nonlinear piezoresistance effects in silicon," *J. Appl. Phys.*, vol. 73, pp. 1838–1847, Aug. 1998. [Online]. Available: https://doi.org/10.1063/1.353169

[8] J. Millán, P. Godignon, X. Perpiñá, A. Pérez-Tomás, and J. Rebollo, "A survey of wide bandgap power semiconductor devices," *IEEE Trans. Power Electron.*, vol. 29, no. 5, pp. 2155–2163, May 2014. [Online]. Available: https://doi.org/10.1109/TPEL.2013.2268900

[9] X. She, A. Q. Huang, Ó. Lucia, and B. Ozpineci, "Review of silicon carbide power devices and their applications," *IEEE Trans. Ind. Electron.*, vol. 64, no. 10, pp. 8193–8205, Oct. 2017. [Online]. Available: https://doi.org/10.1109/TIE.2017.2652401

[10] T. Kimoto, "Material science and device physics in SiC technology for high-voltage power devices," *Jpn. J. Appl. Phys.*, vol. 54, Mar. 2015, Art. no. 40103. [Online]. Available: https://doi.org/10.7567/JJAP.54.040103

[11] T. J. Flack, B. N. Pushpakaran, and S. B. Bayne, "GaN technology for power electronic applications: A review," *J. Electron. Mater.*, vol. 45, pp. 2673–2682, Mar. 2016. [Online]. Available: https://doi.org/10.1007/s11664-016-4435-3

[12] M. Rais-Zadeh *et al.*, "Gallium nitride as an electromechanical material," *J. Microelectromech. Syst.*, vol. 23, no. 6, pp. 1252–1271, Dec. 2014. [Online]. Available: https://doi.org/10.1109/JMEMS.2014.2352617

[13] A. D. Bykhovski, V. V. Kaminski, M. S. Shur, Q. C. Chen, and M. A. Khan, "Piezoresistive effect in wurtzite *n*-type GaN," *Appl. Phys. Lett.*, vol. 68, no. 6, pp. 818–819, Feb. 1996. [Online]. Available: https://doi.org/10.1063/1.116543

[14] J. Richter, J. Pedersen, M. Brandbyge, E. V. Thomsen, and O. Hansen, "Piezoresistance in *p*-type silicon revisited," *J. Appl. Phys.*, vol. 104, no. 2, Jul. 2008, Art. no. 23715. [Online]. Available: https://doi.org/10.1063/1.2960335

[15] C.-H. Cho, R. C. Jaeger, and J. C. Suhling, "Characterization of the temperature dependence of the piezoresistive coefficients of silicon from—150 °C to +125 °C," *IEEE Sensors J.*, vol. 8, no. 8, pp. 1455–1468, Aug. 2008. [Online]. Available: https://doi.org/10.1109/JSEN.2008.923575

[16] Y. P. Varshni, "Temperature dependence of the energy gap in semiconductors," *Physica*, vol. 34, no. 1, pp. 149–154, 1967. [Online]. Available: https://doi.org/10.1016/0031-8914(67)90062-6

[17] G. Xiao, J. Lee, J. J. Liou, and A. Ortiz-Conde, "Incomplete ionization in a semiconductor and its implications to device modeling," *Microelectron. Rel.*, vol. 39, no. 8, pp. 1299–1303, Aug. 1999. [Online]. Available: https://doi.org/10.1016/S0026-2714(99)00027-X

[18] *COMSOL Multiphysics Ver. 5.5*, COMSOL, Stockholm, Sweden, 2019.

[19] H.-P. Phan *et al.*, "Piezoresistive effect in p-type 3C-SiC at high temperatures characterized using Joule heating," *Sci. Rep.*, vol. 6, Jun. 2016, Art. no. 28499. [Online]. Available: https://doi.org/10.1038/srep28499

[20] T.-K. Nguyen *et al.*, "Isotropic piezoresistance of p-type 4H-SiC in (0001) plane," *Appl. Phys. Lett.*, vol. 113, no. 1, Jun. 2018, Art. no. 12104. [Online]. Available: https://doi.org/10.1063/1.5037545

[21] T.-K. Nguyen *et al.*, "Experimental investigation of piezoresistive effect in p-type 4H–SiC," *IEEE Electron Device Lett.*, vol. 38, no. 7, pp. 955–958, Jul. 2017. [Online]. Available: https://doi.org/10.1109/LED.2017.2700402

[22] T. Akiyama, D. Briand, and N. F. de Rooij, "Design-dependent gauge factors of highly doped n-type 4H-SiC piezoresistors," *J. Micromech. Microeng.*, vol. 22, no. 8, Jul. 2012, Art. no. 85034. [Online]. Available: https://doi.org/10.1088/0960-1317/22/8/085034

[23] Z. Li and R. C. Bradt, "Thermal expansion of the hexagonal (4*H*) polytype of SiC," *J. Appl. Phys.*, vol. 60, no. 2, pp. 612–614, Mar. 1986. [Online]. Available: https://doi.org/10.1063/1.337456

[24] A. Arvanitopoulos, N. Lophitis, S. Perkins, K. N. Gyftakis, M. B. Guadas, and M. Antoniou, "Physical parameterisation of 3C-silicon carbide (SiC) with scope to evaluate the suitability of the material for power diodes as an alternative to 4H-SiC," in *Proc. IEEE 11th Int. Symp. Diagan. Electr. Mach. Power Electron. Drives (SDEMPED)*, Tinos, Greece, Aug. 2017, pp. 565–571. [Online]. Available: https://doi.org/10.1109/DEMPED.2017.8062411

[25] C. Darmody and N. Goldsman, "Incomplete ionization in aluminum-doped 4H-silicon carbide," *J. Appl. Phys.*, vol. 126, Oct. 2019, Art. no. 145701. [Online]. Available: https://doi.org/10.1063/1.5120707

[26] M. Roschke and F. Schwierz, "Electron mobility models for 4H, 6H, and 3C SiC [MESFETs]," *IEEE Trans. Electron Devies*, vol. 48, no. 7, pp. 1442–1447, Jul. 2001. [Online]. Available: https://doi.org/10.1109/16.930664

[27] T. Toriyama, "Piezoresistance consideration on n-type 6H SiC for MEMS-based piezoresistance sensors," *J. Micromech. Microeng.*, vol. 14, no. 11, pp. 1445–1448, Aug. 2004. [Online]. Available: https://doi.org/10.1088/0960-1317/14/11/002

[28] J. S. Shor, L. Bemis, and A. D. Kurtz, "Characterization of monolithic n-type 6H-SiC piezoresistive sensing elements," *IEEE Trans. Electron Devices*, vol. 41, no. 5, pp. 661–665, May 1994. [Online]. Available: https://doi.org/10.1109/16.285013

[29] Z. Li, and R. C. Bradt, "Thermal expansion of the hexagonal (6H) polytype of silicon carbide," *J. Amer. Ceram. Soc.*, vol. 69, no. 12, pp. 863–866, Dec. 1986. [Online]. Available: https://doi.org/10.1111/j.1151-2916.1986.tb07385.x

[30] A. A. Lebedev, "Deep level centers in silicon carbide: A review," *Semiconductors*, vol. 33, no. 2, pp. 107–130, Feb. 1999. [Online]. Available: https://doi.org/10.1134/1.1187657

[31] Y. Taki, M. Kitiwan, H. Katsui, and T. Goto, "Electrical and thermal properties of nitrogen-doped SiC sintered body," *J. Jpn. Soc. Powder Powder Metall.*, vol. 65, no. 8, pp. 508–512, Aug. 2018. [Online]. Available: https://doi.org/10.2497/jjspm.65.508

[32] J. S. Shor, D. Goldstein, and A. D. Kurtz, "Characterization of n-type beta -SiC as a piezoresistor," *IEEE Trans. Electron Devices*, vol. 40, no. 6, pp. 1093–1099, Jun. 1993. [Online]. Available: https://doi.org/10.1109/16.214734

[33] F. Iacopi *et al.*, "Orientation-dependent stress relaxation in hetero-epitaxial 3C-SiC films," *Appl. Phys. Lett.*, vol. 102, no. 1, Jan. 2013, Art. no. 11908. [Online]. Available: https://doi.org/10.1063/1.4774087

[34] A. Samanta and I. Grinberg, "Investigation of Si/3C-SiC interface properties using classical molecular dynamics," *J. Appl. Phys.*, vol. 124, no. 17 Nov. 2018, Art. no. 175110. [Online]. Available: https://doi.org/10.1063/1.5042203

[35] D. N. Talwar and J. C. Sherbondy, "Thermal expansion coefficient of 3C-SiC," *Appl. Phys. Lett.*, vol. 67, no. 22, pp. 3301–3303, Nov. 1995. [Online]. Available: https://doi.org/10.1063/1.115227

[36] W. J. Moore, P. J. Lin-Chung, J. A. Freitas Jr., Y. M. Altaiskii, V. L. Zuev, and L. M. Ivanova, "Nitrogen donor excitation spectra in 3C-SiC," *Phys. Rev. B, Condens. Matter*, vol. 48, no. 16, pp. 12289–12291, Oct. 1993. [Online]. Available: https://doi.org/10.1103/physrevb.48.12289

[37] R. Nowak *et al.*, "Elastic and plastic properties of GaN determined by nano-indentation of bulk crystal," *Appl. Phys. Lett.*, vol. 75, no. 14, pp. 2070–2072, Sep. 1999. [Online]. Available: https://doi.org/10.1063/1.124919

[38] M. A. Moram, Z. H. Barber, and C. J. Humphreys, "Accurate experimental determination of the Poisson's ratio of GaN using high-resolution X-ray diffraction," *J. Appl. Phys.*, vol. 102, no. 2, May 2007, Art. no. 23505. [Online]. Available: https://doi.org/10.1063/1.2749484

[39] M. Leszczynski *et al.*, "Thermal expansion of gallium nitride," *J. Appl. Phys.*, vol. 76, no. 8, pp. 4909–4911, Oct. 1994. [Online]. Available: https://doi.org/10.1063/1.357273

[40] T. Haneda, "Basic properties of ZnO, GaN, and related materials," in *Oxide and Nitride Semiconductors*. Berlin, Germany: Springer, 2009, pp. 1–19. [Online]. Available: https://doi.org/10.1007/978-3-540-88847-5_1

[41] G. Sabui, P. J. Parbrook, M. Arredondo-Arechavala, and Z. J. Shen, "Modeling and simulation of bulk gallium nitride power semiconductor devices," *AIP Adv.*, vol. 6, no. 5, Apr. 2016, Art. no. 55006. [Online]. Available: https://doi.org/10.1063/1.4948794

[42] W. Götz, N. M. Johnson, C. Chen, H. Liu, C. Kuo, and W. Imler, "Activation energies of Si donors in GaN," *Appl. Phys. Lett.*, vol. 68, no. 22, pp. 3144–3146, Jun. 1998. [Online]. Available: https://doi.org/10.1063/1.115805

[43] D. A. Neamen, *Semiconductor Physics and Devices*, 4th ed. New York, NY, USA: McGraw-Hill, 2012.

[44] Y. Kanda, "A graphical representation of the piezoresistance coefficients in silicon," *IEEE Trans. Electron Devices*, vol. ED-29, no. 1, pp. 64–70, Jan. 1982. [Online]. Available: https://doi.org/10.1109/T-ED.1982.20659

[45] C. Xiao, D. Yang, X. Yu, L. Xlang, and D. Que, "Determination of the boron and phosphorus ionization energies in compensated silicon by temperature-dependent luminescence," *Silicon*, vol. 9, no. 2, pp. 147–151, May 2014. [Online]. Available: https://doi.org/10.1007/s12633-014-9193-3

[46] M. Forster, A. Cuevas, E. Fourmond, F. E. Rougieux, and M. Lemiti, "Impact of incomplete ionization of dopants on the electrical properties of compensated *p*-type silicon," *J. Appl. Phys.*, vol. 111, no. 4, Feb. 2012, Art. no. 43701. [Online]. Available: https://doi.org/10.1063/1.3686151

[47] T. Toriyama and S. Sugiyama, "Analysis of piezoresistance in *n*-type β-SiC for high-temperature mechanical sensors," *Appl. Phys. Lett.*, vol. 81, no. 15, pp. 2797–2799, Oct. 2002. [Online]. Available: https://doi.org/10.1063/1.1513652

[48] A. Sagar, M. Pollak, and W. Lehmann, "Piezoresistance and piezo-hall effects in *n*-ZnSe," *Phys. Rev.*, vol. 174, no. 3, pp. 859–867, Oct. 1968. [Online]. Available: https://doi.org/10.1103/PhysRev.174.859

[49] C. T. Ser, A. M. Mak, T. Wejrzanowski, and T. L. Tan, "Designing piezoresistive materials from first-principles: Dopant effects on 3C-SiC," *Comput. Mater. Sci.*, vol. 186, Jan. 2021, Art. no. 110040. [Online]. Available: https://doi.org/10.1016/j.commatsci.2020.110040

[50] J. Zhu *et al.*, "Restructured single parabolic band model for quick analysis in thermoelectricity," *NPJ Computat. Mater.*, vol. 7, p. 116, Jul. 2021. [Online]. Available: https://doi.org/10.1038/s41524-021-00587-5

TAKAYA SUGIURA (Member, IEEE) received the B.S., M.S., and Ph.D. degrees in electrical engineering from Keio University, Yokohama, in 2016, 2018, and 2021, respectively, where he is currently a Researcher with the Department of Electronics and Electrical Engineering. His research interests include c-Si solar cells, piezoresistive devices, photonics devices, and power electronics. He has been a member of Electron Devices Society since 2022.

NAOKI TAKAHASHI received the B.S. and M.S. degrees in electrical engineering from Keio University, Yokohama, Japan, in 2019 and 2021, respectively, where he is currently pursuing the master's degree with the School of Integrated Design Engineering, Graduate School of Science and Technology. His research interested include the evaluation of the piezoresistive effect of wide band-gap cubic semiconductor materials using numerical simulations.

RYOHEI SAKOTA received the B.S. degree in electrical engineering from Keio University, Yokohama, in 2021. His research interested include the evaluation of the piezoresistive effect of the silicon carbide material using numerical simulations.

KAZUNORI MATSUDA received the Ph.D. degree from Tsukuba University in 1993. From 2000 to 2003, he collaborated with Prof. Karl Hess's Group in UIUC for simulations on hot carriers and reliability of MOSFET. He is currently a Professor with the Department of Nano Material and Bio Engineering, Tokushima Bunri University. He is currently working on transport phenomena in strained semiconductors and their applications. His research interest includes the wide-bandgap semiconductors.

NOBUHIKO NAKANO (Member, IEEE) was born in 1968. He received the B.S., M.S., and Ph.D. degrees in electrical engineering from Keio University, Japan, in 1990, 1992, and 1995, respectively, where he joined the Department of Electronics and Electrical Engineering, as an Instructor in 1996. He is currently a Professor with the Faculty of Science and Technology, Department of Electronics and Electrical Engineering, Keio University. He is currently working on the design of an on-chip microsystem and bio-medical LSIs. His research interests include LSI/TCAD, numerical simulations, and modeling.